

Magnetic Field Dependence of Magic Numbers in Small Quantum Dots

W.D. Heiss*† and R.G. Nazmitdinov *‡

* Institute for Nuclear Theory, University of Washington, Box 351550, Seattle, WA 98195, USA

† Department of Physics, University of the Witwatersrand, Johannesburg, South Africa

‡ Joint Institute for Nuclear Research, Dubna, Russia

It is argued that various kind of shell structure which occurs at specific values of the magnetic field should be observable in small quantum dots in the addition energies and the magnetic susceptibility.

PACS number(s):73.20Dx, 73.23Ps

Quantum dots are ideal mesoscopic objects for the study of quantum mechanical properties and comparison with classical behavior [1]. The smaller the size of quantum dots, the larger the prevalence of quantum effects upon the static and dynamic properties of these systems. Quantum dots may be considered as true artificial atoms the properties of which can be controlled by men.

An important feature of finite Fermi systems is the existence of shells which give rise to magic numbers. The periodic table of chemical elements is a striking example for the dramatic difference between closed shell and partially filled shell systems; for nuclei and metallic clusters see for example [2–4]. In recent experiments [5–7] shell structure phenomena have been observed clearly for quantum dots. In particular, the energy needed to place the extra electron (addition energy) into a vertical quantum dot has characteristic maxima which correspond to the sequence of magic numbers of a two-dimensional harmonic oscillator [6]. In this Letter we propose manifestations of shell effects that should be observable in the addition energy and the magnetic susceptibility for small quantum dots under the influence of a magnetic field.

We choose as the confining mean field for the electrons in quantum dots the harmonic oscillator potential. Any smooth and finite potential admitting bound states can, for the lowest few levels, generically be approximated by the harmonic oscillator potential [8]. For small electron numbers the harmonic oscillator has been used successfully as a phenomenological effective confining potential in quantum dots [9]. As was shown in the simple case of a two-electron system, the external parabolic potential and the Coulomb interaction leads to a new *oscillator* frequency of the effective mean field [10]. The effect of an external homogeneous magnetic field can be calculated exactly for a three dimensional (3D) harmonic oscillator potential irrespective of the direction of the field [11]. Our discussion here is based upon the 2D version of the Hamiltonian [11]. The magnetic field acts perpendicular to the plane of motion of the electrons and the spin degree of freedom is incorporated, i.e. $H = \sum_{j=1}^N h_j$

where

$$h = \frac{1}{2m^*}(\vec{p} - \frac{e}{c}\vec{A})^2 + \frac{m^*}{2}(\omega_x^2 x^2 + \omega_y^2 y^2) + \mu^* \sigma_z B_z. \quad (1)$$

Here $\vec{A} = [\vec{r} \times \vec{B}]/2$ and σ_z is the Pauli matrix.

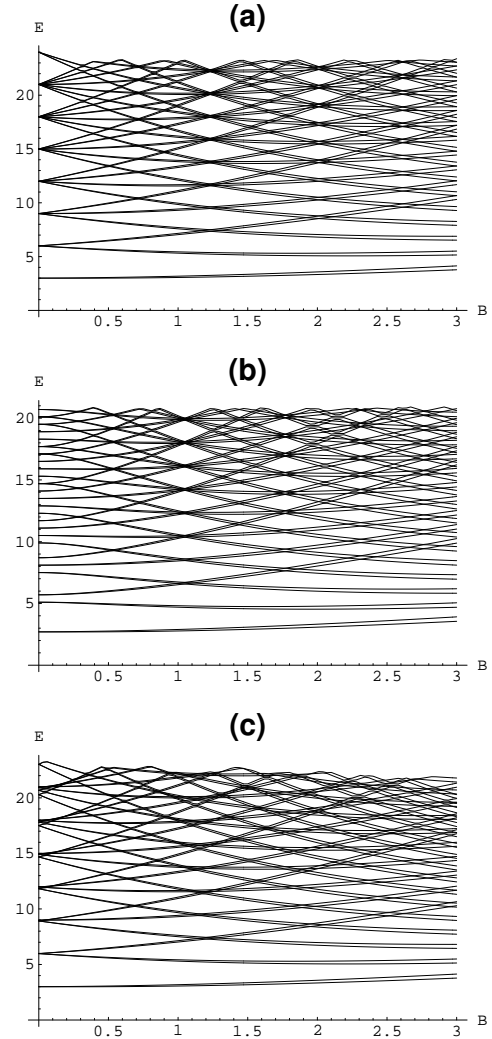


FIG. 1. Single-particle spectra as a function of the magnetic field strength. Spectra are displayed for (a) a plain isotropic two dimensional oscillator, (b) a deformed and (c) an isotropic oscillator including an L^2 -term. For better illustration the value $2\mu^*$ is used for the spin magnetic splitting in all Figures.

We do not take into account the effect of finite temperature; this is appropriate for experiments which are performed at temperatures $kT \ll \Delta$ with Δ being the

mean level spacing. In the following we use meV for the energy and Tesla for the magnetic field strength.

In Fig.1a we display the single-particle spectrum for the isotropic case ($\omega_x = \omega_y$) as a function of the magnetic field strength B . The effective mass which determines the orbital magnetic moment for the electrons is chosen as $m^* = 0.067m_e$. It leads to $\mu_B^{\text{eff}} = 15\mu_B$ while the effective spin magnetic moment is $\mu^* = 0.5\mu_B$. The magnetic orbital effect is much enhanced in comparison with the magnetic spin effect, yet the tiny spin splitting does produce signatures as we see below.

Shell structure occurs whenever the ratio of the two eigenmodes Ω_{\pm} of the Hamiltonian (1) (see Ref. [11]) is a rational number with a small numerator and denominator. The shell structure is particularly pronounced if the ratio is equal to one (for $B = 0$ and $\omega_x = \omega_y$) or two (for $B \approx 1.23$) or three (for $B \approx 2.01$) and lesser pronounced if the ratio is 3/2 (for $B = 0.72$) or 5/2 (for $B = 1.65$). The values given here for B depend on m^* and $\omega_{x,y}$. As a consequence, a material with an even smaller effective mass m^* would show these effects for a correspondingly smaller magnetic field. The magic numbers (including spin) turn out, for $B = 0$, to be the usual sequence of the two dimensional isotropic oscillator, that is $2, 6, 12, 20, \dots$ [6]. For $B \approx 1.23$ we find a new shell structure *as if* the confining potential would be a deformed harmonic oscillator without magnetic field. The magic numbers are $2, 4, 8, 12, 18, 24, \dots$ which are just the numbers obtained from the two dimensional oscillator with $\omega_> = 2\omega_<$ ($\omega_>$ and $\omega_<$ denote the larger and smaller value of the two frequencies). Similarly, we get for $B \approx 2.01$ the magic numbers $2, 4, 6, 10, 14, 18, 24, \dots$ which corresponds to $\omega_> = 3\omega_<$.

If we start from the outset with a deformed mean field, i.e. if we choose, say, $\omega_x = (1 - \beta)\omega_y$ with $\beta > 0$ [12], two major effects are found: (i) the degeneracies (shell structure) are lifted at $B = 0$ depending on the actual value of β , and (ii) the values for B at which the new shell structures occur are shifted to lower values. In Fig.1b we display an example referring to $\beta = 0.2$. The significance of this finding lies in the restoration of shell structures by the magnetic field in an isolated quantum dot that does not give rise to magic numbers at zero field strength due to deformation. We mention that the choice $\beta = 0.5$ would shift the pattern found at $B \approx 1.23$ in Fig.1a to the value $B = 0$.

It is the shell structure caused by the effective mean field which produces the maxima that are observed experimentally in the addition energy $\mu(N+1) - \mu(N) = E_{N+1} - E_N + e^2/C$ [6]. Here E_N is the single-particle energy of the effective mean field in quantum dots, e^2/C is the electrostatic energy and $\mu(N)$ is the chemical potential. The electrostatic energy is much larger than the difference $E_{N+1} - E_N$, however, it is the fluctuations (shell effects) of the difference that matters, at least for small quantum dots [14]. Quantized electronic energies

have been observed even for nanometer-scale metal particles [15]. A similar effect is known in nuclear physics and for metallic clusters. There, shell effects due to single-particle motion create minima in the total potential energy surface which is dominated by the bulk energy, which is the classical liquid drop energy [2–4]. The analogy goes further in that, in an isolated small quantum dot, the external magnetic field acts like the rotation on a nucleus thus creating new shell structure; in this way superdeformation (axis ratio 2:1) has been established for rotating nuclei owing to the shell gaps in the single-particle spectrum [3].

In a previous study [11] we have obtained various shapes of the quantum dot by energy minimization. In this context it is worth noting that at the particular values of the magnetic field, where a pronounced shell structure occurs, the energy minimum would be obtained for circular dots, if the particle number is chosen to be equal to the magic numbers. Deviations from those magic numbers usually give rise to deformed shapes at the energy minimum. To what extent these 'spontaneous' deformations actually occur (which is the Jahn–Teller effect [16]), is subject to more detailed experimental information. The far-infrared spectroscopy in a small isolated quantum dot could be a useful tool to provide pertinent data [11].

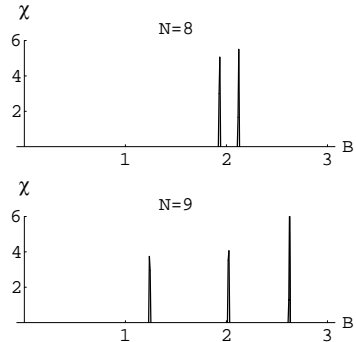


FIG. 2. Magnetic susceptibility $\chi = -\partial^2 E_{\text{tot}} / \partial B^2$ in arbitrary units as a function of the magnetic field strength for the isotropic oscillator without L^2 -term.

The question arises as to what extent our findings depend upon the particular choice of the mean field. Here we confirm the qualitative argument presented above that for sufficiently low electron numbers virtually any binding potential will produce the patterns found for the harmonic oscillator. We add to the Hamiltonian (1) the term $-\lambda\hbar\omega L^2$ where L is the dimensionless z -component of the angular momentum operator. In nuclear physics, the three dimensional analogue of the combined problem is known as the Nilsson model and has been quite successful in explaining the spectra of deformed nuclei [2]. For $\lambda > 0$ the additional term lowers the energy levels of higher angular momenta, in other words, its effect mimics a bulging out of the lower part of the harmonic

oscillator potential. As a consequence, it has the effect of interpolating between the oscillator and the square well single-particle spectrum [3]. For $\omega_x \neq \omega_y$ and $\lambda \neq 0$ the combined Hamiltonian $H' = H - \lambda \hbar \omega L^2$ is non-integrable [13] and the level crossings encountered in Figs.1 become avoided level crossings. The essential effect upon the lower end of the spectrum can be seen in the isotropic oscillator where the magnetic quantum number m is a good quantum number. In this case $H' = H^{\text{isotr}} - \lambda \hbar \omega m^2$.

In Fig.1c we display a spectrum of such H' . The shell structure, which prevails for $\lambda = 0$ throughout the spectrum at $B \approx 1.23$ or $B \approx 2.01$, is now disturbed to an increasing extent with increasing shell number. However, for the parameters chosen the structure is still clearly discernible for about seven shells, that is for particle numbers up to about twenty five. The lifting of the degeneracies at $B = 0$ is also clearly seen where the levels are split according to the absolute values of $|m|$; it is this splitting which gives us guidance in choosing an appropriate value for λ : for $B = 0$ we aim at levels that lie between the corresponding degenerate levels pertaining to the harmonic oscillator and the two dimensional square well where the splitting of these levels is very strong.

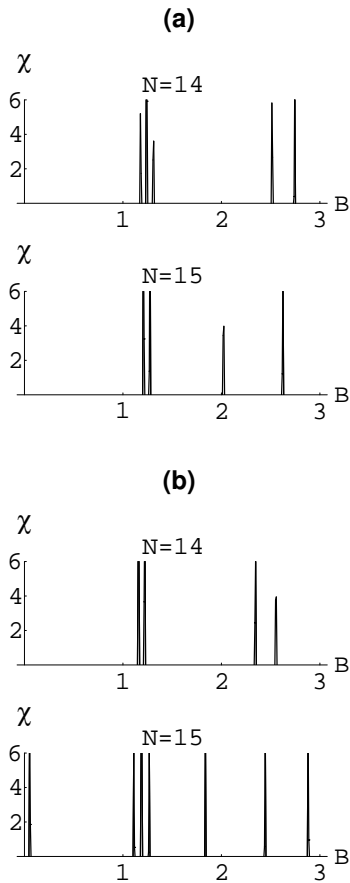


FIG. 3. Similar to Fig.2 for different particle numbers and (a) for $\lambda = 0$ and (b) for $\lambda = 0.01$.

When the magnetic field is changed continuously for a

quantum dot of fixed electron number, the ground state will undergo a rearrangement at the values of B , where level crossings occur. This should be observable in the magnetic susceptibility as it is proportional to the second derivative of the total energy with respect to the field strength. In Figs.2 and 3 we have plotted $-\partial^2 E_{\text{tot}} / \partial B^2$ where E_{tot} is the sum of the single-particle energies filled from the bottom up to N which is the electron number. We discern clearly distinct patterns depending on the electron number, in fact, the susceptibility appears to be a fingerprint pertaining to the electron number. Fig.2 and Fig.3a illustrate results for $\lambda = 0$ and Fig.3b for $\lambda = 0.01$. The deformed oscillator does not produce new features except for the fact that all lines in Figs.2 and 3 would be shifted towards the left in accordance with the discussion above.

All features of Figs.2 and 3 can be understood from the single-particle spectra displayed in Fig.1a and Fig.1c. If there is no level crossing, the second derivative of E_{tot} is a smooth function. The crossing of two occupied levels does not change the smoothness. In contrast, if the last occupied level takes part in a level crossing in such a way that it is ascending before and descending after the crossing, the second derivative of E_{tot} must show a spike. In other words, spikes occur if the last occupied level is bent concavely when viewed from the abscissa; a convex curvature has no effect. As a consequence, we understand the even-odd effect when comparing $N = 8$ with $N = 9$ in Fig.2 and $N = 14$ with $N = 15$ in Fig.3. The spin splitting caused by the magnetic field at $B \approx 2.01$ for $N = 8$ is absent for $N = 9$.

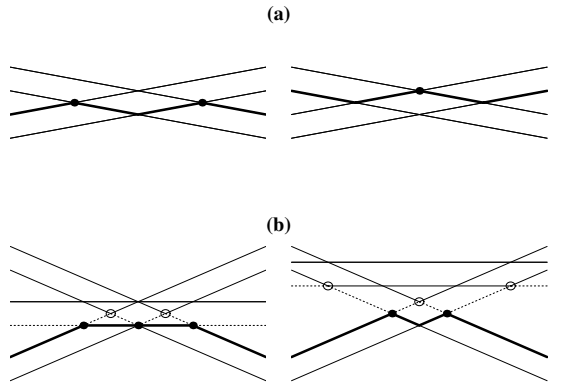


FIG. 4. Blow ups of the relevant level crossings explaining (a) the features in Fig.2 and (b) those of Fig.3. The left and right hand drawing of (a) refers to $N = 8$ and $N = 9$, respectively. The left hand and right hand drawing of (b) refers to $\lambda = 0$ and $\lambda = 0.01$, respectively; here the thick and dotted lines refer to $N = 14$ and $N = 15$.

This becomes evident when looking at a blow up of this particular level crossing which is illustrated in Fig.4a, where the last occupied level is indicated as a thick line and the points where a spike occurs are indicated by a dot. In this way, we also understand that a splitting

occurs for $N = 6$ at $B \approx 1.23$ (not presented here) and no spike at all for $N = 8$ at that same field strength. Note that the splitting is proportional to the effective spin magnetic moment μ^* . Another illustration of the even-odd effect, which persists through all numbers, is given in Fig.3. Now we obtain a triple splitting for $N = 14$ at $B \approx 1.23$ which becomes a double splitting for $N = 15$, while the double splitting for $N = 14$ at $B \approx 2.61$ becomes a single line for $N = 15$. The double splitting is associated with the crossing of only two double lines, while the triple splitting originates from the crossing of three double lines. The line distance at $B \approx 2.61$ is increased as it occurs at a larger field strength.

When we consider the crossing of only two double lines as is the case for $N = 8$ and $N = 9$, or $N = 14$ and $N = 15$ at $B \approx 2.61$, the effect of the L^2 -term is unimportant. However, the L^2 -term does become significant when we turn to level crossings of three or more double lines, in fact, the term removes the artificial pattern of level crossings of three and more lines. We focus our attention at the multiple crossings around $B = 1.2$ by comparing Fig.3a with Fig.3b. In Fig.4b we illustrate a blow up of the situation which produces the different results for $\lambda = 0$ and $\lambda = 0.01$. For $\lambda = 0.01$ the levels with a non-zero slope are lowered as they refer to $m \neq 0$ while the horizontal levels remain unaffected, hence the crossings change as seen by comparing the left and right hand drawing of Fig.4b. The last occupied level is indicated by a thick line and a dotted line for the $N = 14$ and $N = 15$ system, respectively; the corresponding positions, where spikes occur, are marked by solid dots and open circles. The even-odd effect is encountered again but appears converted for $\lambda = 0.01$. Note, however, that the triple line for $N = 15$ at $B = 1.2$ is not a spin splitting but an effect due to the L^2 -term; in other words, for $\mu^* \rightarrow 0$ the double line distance of $N = 14$ in Fig.3b would vanish while the triple line would not as it depends on λ . Spin flips can also be understood by the same token, here the general rule applies: the crossing of the top (bottom) with the bottom (top) line of a double line causes the spin to flip. Hence, both lines of the double splitting in Fig.2 are associated with a spin flip ($N = 8$), but neither of the single lines ($N = 9$). Also, in Fig.3b the triplet ($N = 15$) has no spin flip but if λ would be chosen sufficiently small, the central line of the triplet would be split further and a spin flip would be associated with the doublet (which is then part of a quartet). Strictly speaking, the spikes are δ -functions with a factor which is determined by the angle at which the two relevant lines cross. Our figures are numerical results which do not exactly reflect this feature. If the level crossings are replaced by avoided crossings (Landau-Zener crossings), the lines would be broadened. This would be the case in the present model for $\lambda > 0$ and $\beta > 0$. Finite temperature will also result in line broadening.

To summarize: the consequences of shell structure ef-

fects for the addition energy of a small isolated quantum dot have been analyzed. At certain values of the magnetic field strength shell structures appear in a quantum dot, also in cases where deformation does not give rise to magic numbers at zero field strength. Measurements of the magnetic susceptibility are expected to reflect the properties of the single-particle spectrum and should display characteristic patterns depending on the particle number. The latter property could be of interest in applications because it enables control of the electron number in small isolated quantum dots and the magnetic field strength. The splittings due to the spin magnetic moment provide for a quantitative assessment of the effective spin magnetic moment μ^* .

The authors gratefully acknowledge illuminating discussions with Anupam Garg; fruitful conversations with Yoram Alhassid, Dmitri Averin, Aurel Bulgac and Gregor Hackenbroich are much appreciated. We thank the Department of Energy for its support and the Institute for Nuclear Theory at the University of Washington for its congenial atmosphere.

heiss@physnet.phys.wits.ac.za,
rashid@thsun1.jinr.dubna.su

- [1] M.A. Kastner, Phys.Today **46**, 24 (1993); R.C. Ashoori, Nature (London) **379**, 413 (1996)
- [2] A. Bohr and B.R. Mottelson, *Nuclear Structure* (Benjamin, New York, 1975) Vol.2
- [3] S.G. Nilsson and I. Ragnarsson, *Shapes and Shells in Nuclear Structure* (Cambridge University Press, 1995)
- [4] W.A. de Heer, Rev.Mod.Phys. **65**, 611 (1993); M. Brack, *ibid* **65**, 677 (1993)
- [5] D.J. Lockwood *et al*, Phys.Rev.Lett. **77**, 354 (1996)
- [6] S.Tarucha *et al*, Phys.Rev.Lett. **77**, 3613 (1996)
- [7] M. Fricke *et al*, Europ.Lett. **36**, 197 (1996)
- [8] M. Dineykh and G.V.Efimov, Reports Math.Phys. **36**, 287 (1995)
- [9] D. Heitmann and J. Kotthaus, Phys.Today **46**, 56 (1993)
- [10] M. Dineykh and R.G. Nazmitdinov, Phys.Rev. **B55**, 13707 (1997); cond-mat/9704202
- [11] W.D. Heiss and R.G. Nazmitdinov, Phys.Lett. **A222**, 309 (1996); Phys. Rev. **B55**, N 20 (1997); cond-mat/9704216
- [12] G.Hackenbroich, W.D. Heiss and H.A. Weidenmüller, Phys.Rev.Lett., to appear; cond-mat/9702184
- [13] W.D. Heiss and R.G. Nazmitdinov, Phys.Rev.Lett. **73**, 1235 (1994)
- [14] L.P. Kouwenhoven *et al*, Z. Phys. **B85**, 367 (1991)
- [15] C.T. Black, D.C. Ralph and M. Tinkham, Phys.Rev.Lett. **74**, 3241 (1995); *ibid* **76**, 688 (1996); cond-mat/9701081
- [16] H.A. Jahn and E. Teller, Proc.R.Soc.London, Sec.A **161**, 220 (1937)